

# FIBER ORIENTATION IN INJECTION MOLDED LONG CARBON FIBER THERMOPLASTIC COMPOSITES

Jin Wang<sup>a</sup>, Ba Nghiep Nguyen<sup>b</sup>, Raj Mathur<sup>c</sup>, Bhisham Sharma<sup>d</sup>, Michael D. Sangid<sup>d</sup>,  
Franco Costa<sup>a</sup>, Xiaoshi Jin<sup>a</sup>, Charles L. Tucker III<sup>e</sup>, and Leonard S. Fifield<sup>b</sup>  
<sup>a</sup>Autodesk, Inc., <sup>b</sup>Pacific Northwest National Laboratory, <sup>c</sup>PlastiComp, Inc.,  
<sup>d</sup>Purdue University, <sup>e</sup>University of Illinois at Urbana–Champaign

## Abstract

A set of edge-gated and center-gated plaques were injection molded with long carbon fiber-reinforced thermoplastic composites, and the fiber orientation was measured at different locations of the plaques. Autodesk Simulation Moldflow Insight (ASMI) software was used to simulate the injection molding of these plaques and to predict the fiber orientation, using the Anisotropic Rotary Diffusion and the Reduced Strain Closure models. The phenomenological parameters of the orientation models were carefully identified by fitting to the measured orientation data. The fiber orientation predictions show very good agreement with the experimental data.

## Introduction

Challenged by the new fuel-economy requirements of vehicles, the automobile industry is seeking lightweight structural materials without sacrificing vehicle safety and durability. Long carbon fiber-reinforced polymer composites (LCFRP) are gaining increased interest for automakers around the world, owing to their high strength-to-weight ratio and high corrosion resistance. Vehicle fuel-economy can be significantly increased by replacing steel parts with LCFRP. However, the strength and performance of LCFRP parts strongly depend on the fiber orientation and fiber length induced by the polymer flow during processing, most commonly injection molding. For example, the strength of a LCFRP part is higher in the direction along which the majority of fibers are aligned than in the other directions. The complex preferential orientation of fibers in an injection-molded part is the result of the interactions of part design, tool design, processing condition, and material. A predictive engineering tool for the fiber orientation is valuable for the design and production of parts with desirable performance.

Computational simulation software for injection molding has been utilized widely to aid part and tool design and the selection of processing conditions and materials. To calculate the fiber orientation during the injection molding process, most software uses the Folgar-Tucker model [1], which follows the Jeffery's equation [2] for the motion of a single cylindrical rigid particle and

adds a phenomenological isotropic rotary diffusion term to represent the fiber-fiber interactions. The equation is recast in terms of the second-order orientation tensor for its simplicity and affordable computations. Recent experiments have shown that the rate of fiber orientation development is slower than the Folgar-Tucker model predicts and the overall fiber alignment is weaker than predicted. Wang et al. [3] modified the Folgar-Tucker model by reducing the growth rates of the eigenvalues of the fiber orientation tensor by a constant scalar factor while keeping the rotation rates of the eigenvectors unchanged. Thus was developed the *Reduced Strain Closure* (RSC) model. The RSC model exhibits slower orientation kinetics than the Folgar-Tucker model but a similar steady-state orientation. The RSC model has been validated against fiber orientation measurements for short fiber-reinforced polymer composites (SFRP) and provides excellent agreement with experiment [4, 5].

However, the Folgar-Tucker and RSC models are less accurate for long fiber-reinforced composites (LFRP), because in LFRP the fiber alignment in the flow direction is normally lower than in SFRP. The isotropic rotary diffusion used in the Folgar-Tucker and RSC models are unable to capture the behavior of interactions between long fibers and fail to accurately predict all diagonal fiber orientation components simultaneously. As proposed by Phelps et al. [6], this isotropic diffusion can be replaced by *anisotropic rotary diffusion* (ARD), which is defined on the surface of the unit sphere traced by all orientations of the unit vector. The ARD model combined with the RSC model has been applied to accurately predict the orientation for injection-molded long glass fiber composites [6 – 8].

This work is part of the predictive engineering project for injection-molded long carbon fiber composites, sponsored by the US Department of Energy. ASMI is used to simulate the injection molding and predict the orientation of long carbon fibers, using the ARD and RSC models. The results are compared to experimental measurements.

## Fiber Orientation Models

The orientation of a single rigid fiber can be described by a unit vector  $\mathbf{p}$  along the fiber axis. For collections of fibers, the general and concise description is to use the second-order orientation tensor,  $\mathbf{A} = \langle \mathbf{p}\mathbf{p} \rangle$ , which is defined as the average of the dyadic product of  $\mathbf{p}$ . The second-order orientation tensor  $\mathbf{A}$  is symmetric and has a trace equal to 1 owing to the normalization condition.

The widely used Folgar-Tucker model is written in the terms of the second-order tensor  $\mathbf{A}$  as [1]

$$\frac{D\mathbf{A}}{Dt} = (\mathbf{W} \cdot \mathbf{A} - \mathbf{A} \cdot \mathbf{W}) + \zeta(\mathbf{D} \cdot \mathbf{A} + \mathbf{A} \cdot \mathbf{D} - 2\mathbb{A}:\mathbf{D}) + 2C_I\dot{\gamma}(\mathbf{I} - 3\mathbf{A}). \quad (1)$$

Here,  $DA/Dt$  is the material derivative of  $\mathbf{A}$ ;  $\mathbf{W}$  and  $\mathbf{D}$  are the anti-symmetric and symmetric parts of the velocity gradient tensor, respectively, and  $\dot{\gamma}$  is the scalar magnitude of  $\mathbf{D}$ ;  $\zeta$  is the particle shape parameter and is very close to unity due to the high length-to-radius ratio of fibers.  $\mathbb{A}$  is the fourth-order orientation tensor, defined as  $\mathbb{A} = \langle \mathbf{p}\mathbf{p}\mathbf{p}\mathbf{p} \rangle$ , and is approximated by a closure function of the components of  $\mathbf{A}$ . The last term on the right-hand side is the isotropic diffusion term and  $C_I$  is the interaction coefficient. A larger  $C_I$  implies stronger fiber-fiber interactions. For a given flow, the steady-state solution of the orientation equation is controlled by the  $C_I$  value.

The RSC model reduces the kinetic rate of fiber orientation development in an objective fashion and is written as [3]

$$\begin{aligned} \frac{D\mathbf{A}}{Dt} = & (\mathbf{W} \cdot \mathbf{A} - \mathbf{A} \cdot \mathbf{W}) + \zeta(\mathbf{D} \cdot \mathbf{A} + \mathbf{A} \cdot \mathbf{D}) \\ & - 2[\mathbb{A} + (1 - \kappa)(\mathbb{L} - \mathbb{M}:\mathbb{A}):\mathbf{D}] \\ & + 2\kappa C_I\dot{\gamma}(\mathbf{I} - 3\mathbf{A}). \end{aligned} \quad (2)$$

Here the fourth-order tensor  $\mathbb{M} = \sum_{i=1}^3 \mathbf{e}_i \mathbf{e}_i \mathbf{e}_i \mathbf{e}_i$  and  $\mathbf{e}_i$  ( $i=1, 2, 3$ ) are the eigenvectors of the orientation tensor  $\mathbf{A}$ , and the fourth-order tensor  $\mathbb{L} = \mathbb{M} \cdot \mathbf{A}$ . The scalar factor  $\kappa$  is a phenomenological parameter and its value is determined by fitting the fiber orientation or rheology prediction to experiments. A typical value of  $\kappa$  ranges from 0.01 to 0.1, and the smaller the value, the slower the orientation development rate. Setting  $\kappa = 1$  reduces the RSC model of Eq. (2) to the Folgar-Tucker model of Eq. (1).

The ARD model was developed for LFRP and the RSC version of the ARD model (ARD-RSC) is

$$\begin{aligned} \frac{D\mathbf{A}}{Dt} = & (\mathbf{W} \cdot \mathbf{A} - \mathbf{A} \cdot \mathbf{W}) + \zeta(\mathbf{D} \cdot \mathbf{A} + \mathbf{A} \cdot \mathbf{D}) \\ & - 2[\mathbb{A} + (1 - \kappa)(\mathbb{L} - \mathbb{M}:\mathbb{A}):\mathbf{D}] \\ & + \dot{\gamma}[2[\mathbf{C} - (1 - \kappa)\mathbb{M}:\mathbf{C}] - 2\kappa(\text{tr}\mathbf{C})\mathbf{A} \\ & - 5(\mathbf{C} \cdot \mathbf{A} + \mathbf{A} \cdot \mathbf{C}) \\ & + 10[\mathbb{A} + (1 - \kappa)(\mathbb{L} - \mathbb{M}:\mathbb{A}):\mathbf{C}]. \end{aligned} \quad (3)$$

Here, the rotary diffusion tensor  $\mathbf{C}$  is constructed from  $\mathbf{A}$  and  $\mathbf{D}$  to be objective, as

$$\mathbf{C} = b_1\mathbf{I} + b_2\mathbf{A} + b_3\mathbf{A}^2 + b_4\frac{\mathbf{D}}{\dot{\gamma}} + b_5\frac{\mathbf{D}^2}{\dot{\gamma}^2}, \quad (4)$$

where  $b_i$  ( $i = 1, \dots, 5$ ) are scalar constants and must be carefully selected by matching to measured steady-state orientation and requiring a stable orientation solution. Setting  $b_1 = C_I$  and  $b_i = 0$  ( $i = 2, \dots, 5$ ) reduces the ARD-RSC model of Eq. (3) to the RSC model of Eq. (2).

In a thin injection-molded part, the fiber orientation through the thickness normally shows a shell/core/shell structure, as illustrated in Fig. 1. Near the part surface, the shearing deformation is dominant in the polymer flow and aligns fibers in the flow direction, but due to the inter-fiber interactions, i.e., the diffusion in the fiber orientation model, fibers are not perfectly aligned. These regions are referred to as *shell* layers. Near the center of the thickness cross-section, fibers are strongly aligned in the cross-flow direction or randomly aligned in the part plane, dependent on the flow type during the injection molding. This region is referred to as the *core*. Compared to SFRPs, LFRPs normally exhibit a thicker core and weaker alignment in the flow direction in the shell layers. In a flat part, most fibers lie in the plane and the orientation component in the thickness direction is very small.

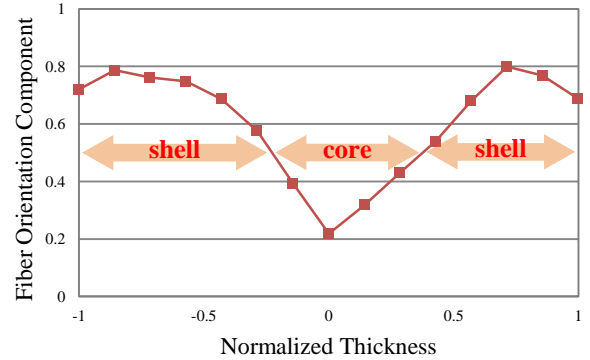


Figure 1. Typical shell/core/shell structure of the fiber orientation through the thickness in a thin injection-molded part.

In general, given a sufficiently long flow length, the orientation in the shell layers reaches its steady-state equilibrium solution. In such a case, the model prediction in the shell layers is controlled by the isotropic interaction coefficient  $C_I$  in Eqs. (1) and (2) or the anisotropic rotary diffusion tensor  $\mathbf{C}$  in Eq. (3). The orientation in the core, where the accumulated shear deformation is lower, corresponds to the transient solution of the orientation equation. Since it over-predicts the rate of orientation change, the Folgar-Tucker model normally over-predicts the flow-direction alignment in the core, which results in a narrower core than observed in experiments. The RSC model corrects the over-prediction problem by reducing

the rate of orientation change. Normally, as the scalar factor  $\kappa$  decreases the core width increases.

## Injection Molding and Measurements

Two 178 mm  $\times$  178 mm  $\times$  3.175 mm (7"  $\times$  7"  $\times$  1/8") plaques were molded with polypropylene reinforced with 50-wt% long carbon fiber (LCF) by PlastiComp, Inc. One plaque was molded with an edge gate and the other with a center gate, as illustrated in Figs. 2 – 3, respectively. The nominal length of carbon fibers was 12 mm.

A system of fiber orientation measurement was developed by Purdue University [9]. Three 23 mm  $\times$  23 mm (0.9"  $\times$  0.9") samples were cut at different locations along the centerline from each injection-molded plaque, and they were labeled as A, B, and C from near the gate to the part end, as illustrated in Figs. 2 and 3. The cross-section of each sample was polished and the digitized images were captured. An automated image analysis program performed an edge detection algorithm to fit an ellipse on each fiber's cross-section, and calculated the second-order orientation tensor.

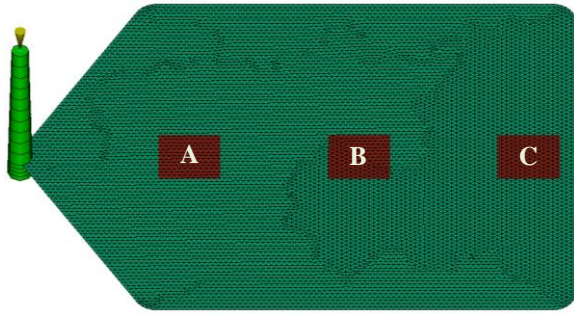


Figure 2. Model and mesh of the edge-gated plaque, and locations for measurement samples.

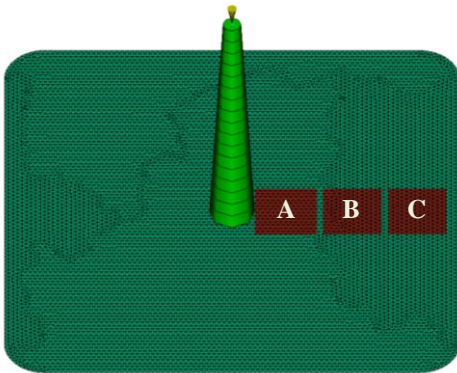


Figure 3. Model and mesh of the center-gated plaque, and locations for measurement samples.

## Simulations

The ASMI 2015 software was used to simulate the injection molding process and to predict the fiber

orientation in the plaques. The parts were modeled with midplane meshes and the sprue with beam elements, as shown in Figs. 2 and 3 for the edge-gated and center-gated plaques, respectively. A midplane mesh in ASMI consists of layered triangular shell elements.

The  $b_i$  parameters in the ARD model were identified following the procedure proposed by Phelps et al. [6], by fitting the steady-state solution in a simple shear flow to a selected target orientation and requiring a physically valid tensor  $\mathbf{C}$  in all flows and stable transient orientation solutions in simple shear as well as planar, uniaxial, and biaxial elongation flows. The target steady-state fiber orientation was chosen based on the medium measured orientation in shell layers of all measured samples, which for the 50-wt% LCF/PP used in this work is

$$\mathbf{A}^{\text{SS}} = \begin{bmatrix} 0.72 & 0 & 0.04 \\ 0 & 0.21 & 0 \\ 0.04 & 0 & 0.01 \end{bmatrix}. \quad (5)$$

The resulting model parameters were  $b_i = [0.001654, 0.0054, 0.025, -0.0008676, -0.005]$ . The scalar factor  $\kappa$  of the RSC model was chosen as 0.02. The fiber orientation inlet condition applied at the gate was selected such that the orientation prediction reasonably matches the experimental data at location A.

## Results and Discussion

The ASMI prediction of fiber orientation is compared to the experimental results in Figs. 4 – 6 for the edge-gated plaque and in Figs. 7 – 9 for the center-gated plaque. Here  $A_{11}$  denotes the component of the fiber orientation tensor in the flow direction, and  $A_{22}$  denotes the component in the cross-flow direction. These two diagonal components represent the strength of fiber alignment in the respective directions.

The experimental data exhibit a wider core in the center-gated plaque than in the edge-gated plaque due to the different flow patterns in the respective parts. In the edge-gated plaque, the flow front is flat and the flow pattern is unidirectional in the measurement regions, so simple shear flow is dominant in most of the cavity. In the center-gated plaque the radial flow pattern results in a combination of simple shear flow and planar elongation flow. The elongation flow is dominant near the gate and near the center of the thickness. This aligns fibers in the stretching direction, which is the cross-flow direction in a radial flow. The ASMI predictions using the ARD-RSC model show very good agreement with the experimental orientation data at all locations for both edge-gated and center-gated plaques.

With the RSC factor  $\kappa = 0.02$ , the ASMI software predicts the core width very well in both plaques. Along the flow path from locations A to B to C, the core

becomes narrower in the measured orientation data, as the shearing flow gradually aligns more fibers in the flow direction. The predictions correctly capture this trend.

The shell layers are very thin because the core is very thick in these LCFRP parts. The shell layers are much thinner in the center-gated plaque than in the edge-gated plaque. This is likely because the flow length in the former is half of the flow length of the latter and fibers in the shell layers do not have as much time to become aligned in the flow direction by the simple shear flow. This is also correctly captured by the ASMI predictions. In the shell layers of the edge-gated plaque, the orientation prediction is close to the steady-state solution of the ARD model. Since the medium values of shell orientation data from all locations of both plaques were used as the target orientation to fit the model parameter, ASMI slightly under-predicts  $A_{11}$  and over-predicts  $A_{22}$  in shell layers in locations A and B, and vice versa in location C. In the center-gated plaque, ASMI also slightly under-predicts  $A_{11}$  and over-predicts  $A_{22}$  in one shell layer ( $z > 0$ ) in locations A and B, but the prediction is very good in location C.

The orientation data also exhibits asymmetry about the mid-thickness plane ( $z = 0$ ), especially near the part surface in the center-gated plaque. This could be due to the asymmetric flow as the polymer melt enters the cavity from one side. In the ASMI midplane model, the flow representation is symmetric about the mid-thickness plane, thus the fiber orientation prediction is also symmetric. Overall, the predictions of orientation distribution through the thickness agree well with the measured data.

## Conclusions

The fiber orientation in injection molded LCFRP was studied. The measured orientation data through the thickness exhibit a very thick core and thin shell layers. The phenomenological parameters in the fiber orientation models, including the  $b_i$  parameters in the ARD model and the  $\kappa$  factor in the RSC model, were identified by fitting the model predictions to the experimental data. The good agreement between the ASMI orientation predictions and the measured orientation data supports the usefulness of the ARD-RSC model for LCFRP. Accurate prediction of fiber orientation is crucial for the subsequent prediction of the fiber length distribution and mechanical properties for structural analyses.

## Acknowledgements

The authors would like to thank the US Department of Energy for sponsoring the Predictive Engineering Tools project on Long-Carbon-Fiber Thermoplastic Composites. In addition, this work was performed under CRADA No.

336 between Battelle as Operator of Pacific Northwest National Laboratory, Autodesk, Inc., Toyota Motor Engineering & Manufacturing North America, and Magna Exteriors & Interiors Corp.

## References

1. S. G. Advani and C. L. Tucker III. "The Use of Tensors to Describe and Predict Fiber Orientation in Short Fiber Composites." *Journal of Rheology* **31**: 751–784 (1987).
2. G. B. Jeffery. "The Motion of Ellipsoidal Particles Immersed in a Viscous Fluid." *Proceedings of the Royal Society* **A102**: 161–179 (1922).
3. J. Wang, J. F. O’Gara, and C. L. Tucker III. "An Objective Model for Slow Orientation Kinetics in Concentrated Fiber Suspensions: Theory and Rheological Evidence." *Journal of Rheology* **52**(5): 1179–1200 (2008).
4. J. Wang. "Improved Fiber Orientation Predictions For Injection-molded Composites." *Ph.D Thesis, University of Illinois at Urbana-Champaign, Urbana, IL* (2007).
5. J. Wang and X. Jin. "Comparison of Recent Fiber Orientation Models in Autodesk Moldflow Insight Simulations with Measured Fiber Orientation Data." *Polymer Processing Society 26th Annual Meeting* (2010).
6. J. Phelps and C. L. Tucker III. "An Anisotropic Rotary Diffusion Model for Fiber Orientation in Short- and Long-Fiber Thermoplastics." *Journal of Non-Newtonian Fluid Mechanics* **156**(3): 165–176 (2009).
7. B. N. Nguyen, X. Jin, J. Wang, V. Kunc, and C. L. Tucker III. "Validation of New Process Models for Large Injection-Molded Long-Fiber Thermoplastic Composite Structures." *PNNL-21165, Pacific Northwest National Laboratory* (2012).
8. S. Han, X. Jin, J. Wang, F. Costa, and R. Bendickson. "The Three Dimensional Numerical Analysis and Validation of Compression Molding Process." *SPE ANTEC* (2012).
9. B. N. Nguyen, S. E. Sanborn, R. N. Mathur, B. Sharma, M. D. Sangid, J. Wang, X. Jin, F. Costa, U. N. Gandhi, S. Mori, and C. L. Tucker III. "Predictive Engineering Tools for Injection-molded Long-Carbon-Fiber Thermoplastic Composites - FY 2014 Third Quarterly Report". *PNNL-23499, Pacific Northwest National Laboratory* (2014).

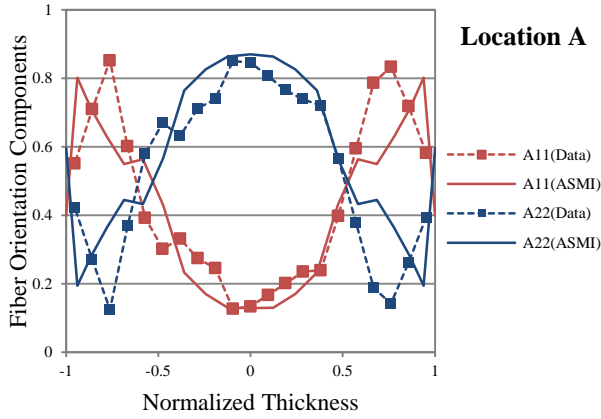


Figure 4. Comparison of fiber orientation data with ASMI predictions at location A of the edge-gated plaque.

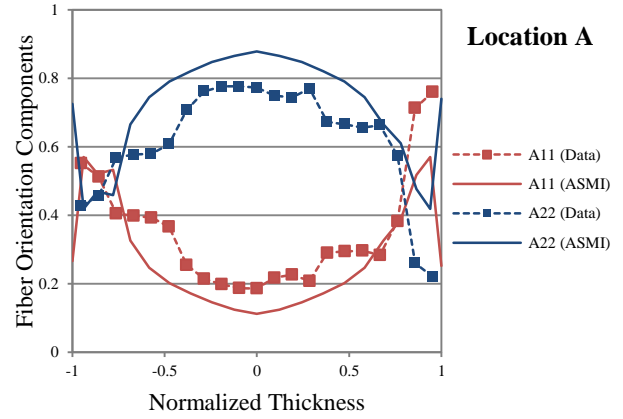


Figure 7. Comparison of fiber orientation data with ASMI predictions at location A of the center-gated plaque.

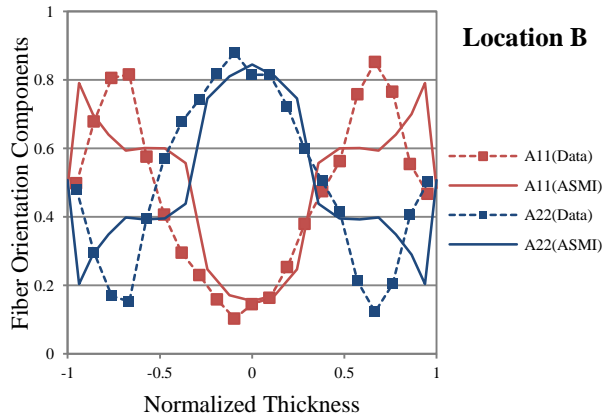


Figure 5. Comparison of fiber orientation data with ASMI predictions at location B of the edge-gated plaque.

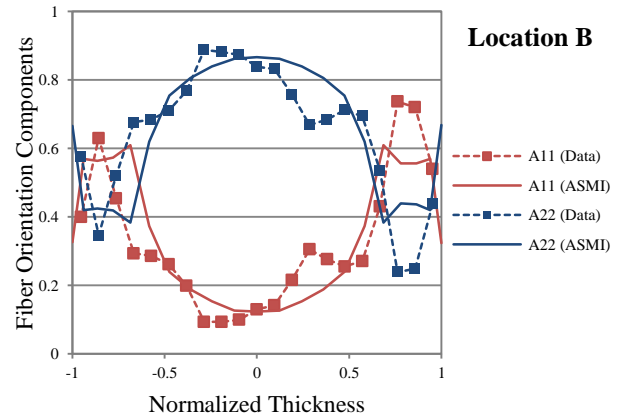


Figure 8. Comparison of fiber orientation data with ASMI predictions at location B of the center-gated plaque.

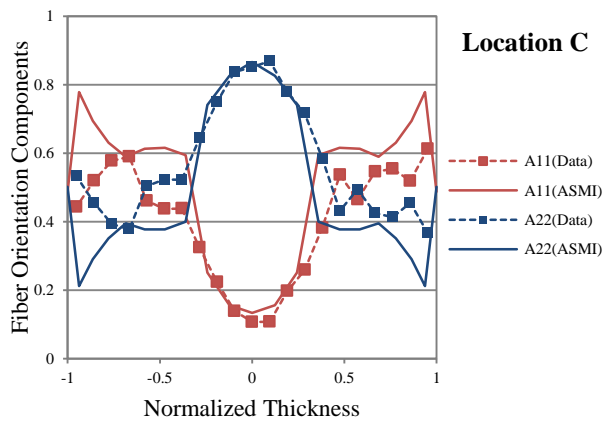


Figure 6. Comparison of fiber orientation data with ASMI predictions at location C of the edge-gated plaque.

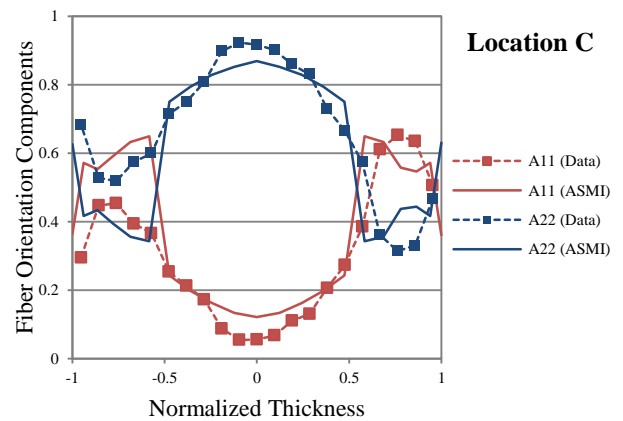


Figure 9. Comparison of fiber orientation data with ASMI predictions at location C of the center-gated plaque.